FT-IR Studies on the Triplet State of P_{680} in the Photosystem II Reaction Center: Triplet Equilibrium within a Chlorophyll Dimer†

Takumi Noguchi,*,‡ Yorinao Inoue,‡ and Kimiyuki Satoh§

Solar Energy Research Group, The Institute of Physical and Chemical Research (RIKEN), Wako, Saitama 351-01, Japan, and Department of Biology, Faculty of Science, Okayama University, Tsushima-naka, Okayama 700, Japan

Received January 11, 1993; Revised Manuscript Received April 12, 1993

ABSTRACT: The structure and molecular interactions of the primary donor (P_{680}) in the reaction center (D1–D2–cytochrome *b*–559 complex) of photosystem II (PS II) have been investigated by detecting light-induced FT-IR difference spectra upon the formation of its triplet state ($^3P_{680}$). The $^3P_{680}/P_{680}$ spectrum obtained was analyzed by comparing it with difference spectra between the ground and lowest triplet states of purified chlorophyll *a* (Chl) in organic solvents. The negative peaks at 1669 and 1707 cm^{-1} accompanied by the positive peaks at 1627 and 1659 cm^{-1} in the $^3P_{680}/P_{680}$ spectrum were assigned to the keto C=O stretching mode, and the appearance of these two pairs of bands indicated that P_{680} has a dimeric structure analogous to that of the bacterial primary donor. From the band positions of the keto and carbomethoxy C=O stretches, the hydrogen-bonding properties of these two Chl molecules were found to be asymmetrical; in one Chl molecule both the keto and carbomethoxy C=O groups form hydrogen bonds, while in the other Chl molecule the keto C=O is not hydrogen-bonded whereas the carbomethoxy C=O probably is hydrogen-bonded. The temperature dependence of the intensity ratios of the keto C=O bands revealed that the triplet state is equilibrated between the two Chl molecules with an energy gap of 8.4 ± 0.7 meV. Most of the triplet population was found to be localized on one Chl molecule (86% at 80 K), in which both of the two C=O groups are hydrogen-bonded, that is probably attached to the D1 subunit. Considering the structure of the bacterial reaction center determined by X-ray crystallography and the sequence homology between the D1 and D2 subunits of PS II and the L and M subunits of bacteria, a model of the P_{680} structure and its interactions with apoproteins has been proposed.

Higher plants, eukaryotic algae, and cyanobacteria utilize a combined function of two photosystems, photosystem I (PS I)[1] and photosystem II (PS II), in the conversion of light energy to chemical energy. As for PS II, the reaction center (RC), where the initial charge separation and the subsequent electron-transfer reactions are carried out, consists of the so-called D1 and D2 polypeptides, which was demonstrated by the isolation of a photochemically active D1–D2–cyt *b*–559 complex (Nanba & Satoh, 1987; Barber et al., 1987). It has been proposed that the RC and PS II is analogous to that of photosynthetic bacteria, whose structure has been clarified by X-ray crystallography (Deisenhofer et al., 1984, 1985; Michel et al., 1986; Allen et al., 1987a,b; Yeates et al., 1988; Change et al., 1991; El-Kabbani et al., 1991). Amino acid sequences of the D1 and D2 subunits have homology with the L and M subunits of bacterial RC, respectively (Trebst, 1986; Sayre et al., 1986; Michel & Deisenhofer, 1988), and the redox components and the electron-transfer pathways also are almost identical, i.e., the primary donor (bacterio)-chlorophyll ((B)Chl) gives rise to charge separation and an electron is transferred to (bacterio)pheophytin ((B)Pheo), the primary quinone acceptor (Q_A), and further to the secondary quinone acceptor (Q_B).

Among these redox components, the primary donor plays the essential role as a reaction initiator for the consequent photosynthetic processes. The primary donor of bacterial RC is known to form a dimeric structure called the special pair, in which a pair of BChl molecules symmetrically arrange in parallel, overlapping each other in ring I (Deisenfoher et al., 1984; Allen et al., 1987a). This arrangement causes a strong exciton coupling, resulting in a large splitting of the far-red absorption bands [reviewed in Friesner and Won (1989)].

The overall similarity between PS II and bacterial RCs mentioned above and, in particular, the fact that the two histidine residues ligating to the bacterial special pair are conserved in the D1 and D2 subunits (Trebst, 1986; Sayre et al., 1986; Michel & Deisenhofer, 1988) naturally lead to a model of the PS II primary donor (P_{680}) having a dimeric structure. In fact, several studies have argued this subject in favor of the dimeric structure (Van Gorkom et al., 1974; Den Blanken et al., 1983; Van Kan et al., 1990; Braun et al., 1990; Durrant et al., 1990; Kwa et al., 1992; Otte et al., 1992).

Nevertheless, a considerable number of studies has shown the monomeric nature of P_{680}: the redox potential as high as that of *in vitro* monomeric Chl (Davis et al., 1979), the small or no band splitting in red absorption (Tetenkin et al., 1989; Van der Vos et al., 1992), the small Stark effect (Lösche et al., 1988), the values of zero-field splitting parameters of the

† This work was supported by a grant for Photosynthetic Sciences at The Institute of Physical and Chemical Research (RIKEN) given by the Science and Technology Agency (STA) of Japan to T.N. and Y.I., by a grant from Mitsubishi Foundation, and by a Grant-in-Aid for Scientific Research of Priority Areas (No. 04273101) from the Ministry of Education, Science and Culture of Japan to K.S.

* Author to whom correspondence should be addressed.

‡ The Institute of Physical and Chemical Research (RIKEN).

§ Okayama University.

[1] Abbreviations: PS I, photosystem I; PS II, photosystem II; RC, reaction center; Cyt, cytochrome; BChl, bacteriochlorophyll *a*(*b*); Chl, chlorophyll *a*; BPheo, bacteriopheophytin *a*(*b*); Pheo, pheophytin *a*; Q_A, primary quinone acceptor; Q_B, secondary quinone acceptor; P_{680}, primary electron donor of photosystem II; $^3P_{680}$, lowest excited triplet state of P_{680}; ESR, electron spin resonance; FT-IR, Fourier transform infrared; S_0, ground singlet state; T_1, lowest excited triplet state; SDS, sodium dodecyl sulfate; THF, tetrahydrofuran; TEA, triethylamine; EtOH, ethanol; ADMR, absorbance-detected magnetic resonance.

0006-2960/93/0432-7186$04.00/0 © 1993 American Chemical Society

$^3P_{680}$ ESR spectrum similar to those of monomeric Chl (Rutherford et al., 1981; Ghanotakis et al., 1989), the triplet z axis significantly tilted to be approximately parallel to the membrane plane as the accessory BChl in bacterial RC (Rutherford, 1985; Van Mieghem et al., 1991), and the observation of bleaching only a single keto C=O band upon $^3P_{680}$ formation in the resonance Raman spectrum (Moënne-Loccoz et al., 1990). Thus, the final conclusion about the P_{680} structure is left to be drawn by other spectroscopic methods.

Fourier transform infrared (FT-IR) difference spectroscopy has the advantage of detecting small structural changes of reactive molecules in large proteins [reviewed in Lutz and Mäntele (1991)]. This spectroscopy can also provide much more direct information about molecular structures and interactions than electronic absorption or ESR spectroscopies. In particular, C=O stretching modes, which appear strongly in IR spectra, are significantly sensitive to such molecular environments as hydrogen-bonding interactions (Katz et al., 1966; Bekarek et al., 1979; Koyama et al., 1986; Krawczyk, 1989), so that we can make a good use of the relatively narrow IR bands in distinguishing the individual Chl molecules existing in different environments. Furthermore, some of the macrocycle C=C stretching modes are known as good diagnoses to determine the coordination state of central Mg (Fujiwara & Tasumi, 1986; Tasumi & Fujiwara, 1987; Tasumi, 1989).

In the D1–D2–cyt b–559 complex, Q_A is lacking, and hence the charge-separated state, $P_{680}^+Pheo^-$, immediately recombines to form $^3P_{680}$ with high efficiencies at low temperatures (Takahashi et al., 1987). Since the resultant $^3P_{680}$ has a relatively long lifetime (~1 ms) (Takahashi et al., 1987), $^3P_{680}$ accumulates under continuous-light illumination. In this study, we have utilized this $^3P_{680}$ formation and measured light-induced FT-IR difference spectra between P_{680} and $^3P_{680}$ for the purpose of clarifying the structure of P_{680} and its interaction with apoproteins. In order to analyze the $^3P_{680}/P_{680}$ spectra obtained, we further measured the FT-IR difference spectra of *in vitro* Chl between the ground singlet state (S_0) and the lowest excited triplet state (T_1) in various solvents. The results indicated that P_{680} has a dimeric structure and its triplet state is equilibrated among the two Chl molecules, each of which has different hydrogen-bonding properties.

MATERIALS AND METHODS

The D1–D2–cyt b–559 complex was purified from spinach grana thylakoids according to Nanba and Satoh (1987), with modifications which include isoelectric focusing in the presence of dodecyl maltoside. The RC sample in 50 mM Tris buffer (pH 7.2) including 0.2% dodecyl maltoside was stored at −80 °C until measurement. As for the samples for FT-IR measurements, the buffer system was replaced by 10 mM phosphate buffer (pH 7.2) in order to diminish the IR bands of the buffer in the region between 1000 and 1800 cm^{-1}. For H–D exchange experiments, RC dissolved in a phosphate–D_2O buffer was incubated at 4 °C for a day. Denaturation of the RC complex was carried out by adding 1% sodium dodecyl sulfate (SDS) to the sample solution followed by incubation at 40 °C for 10 min. Chl was extracted from spinach and purified according to the method of Omata and Murata (1980). In order to remove water, the solid Chl sample was dried at 70 °C under vacuum for 1 h.

For FT-IR measurements of RC, a 15-μL aliquot of the sample solution (1.2 mg Chl/mL) was put on a BaF_2 plate (13 mm diameter) and lightly dried under an N_2 gas stream. The resultant RC film was pressed with another BaF_2 plate and then set in a cryostat. The absorbance of this RC sample was 0.7 at 1656 cm^{-1} (amide I band). For measurements of purified Chl, Chl dissolved in tetrahydrofuran (THF), triethylamine (TEA), or ethanol (EtOH) at 10^{-2} M was injected between a pair of BaF_2 plates whose light path length was controlled to be about 50 μm with a few layers of aluminum foil as a spacer. The absorbances of typical Chl bands appearing at 1650–1750 cm^{-1} (C=O stretching modes) were 0.2–0.3.

FT-IR spectra were measured on a JEOL JIR-6500 spectrophotometer equipped with an MCT detector (EG&G JUDSON IR-DET101). The sample temperature was controlled with a cryostat (Oxford DN1704) equipped with a temperature control unit (Oxford ITC-4). In order to cut the visible light contaminating the IR beam and to protect the detector from the excitation white light, one of a pair of Ge filters (OCLI LO2584-9) was placed before and one behind the sample. Light-induced difference spectra were obtained by subtracting the single-beam spectrum taken before illumination from that taken under illumination or that taken after illumination. The single-beam spectra before illumination were accumulated for 200 scans (100 s), and the spectra under and after illumination were accumulated for 10 scans (5 s). The shorter accumulation time for the under and after illumination spectra was necessary to minimize the temperature rise due to light illumination (see Results). The final spectrum was obtained by averaging 10 spectra. The difference spectrum due to the temperature rise was obtained as a subtraction between the two single-beam spectra (200 scans for each) taken while the temperature was increased from 80 to 81 K. The resolution of all of the spectra was 4 cm^{-1}.

ESR spectra were recorded with a JEOL ES-FE1XG X-band EPR spectrometer equipped with a liquid N_2 cryostat (JEOL ES DVT-1). The spectrum of the T_1 state of Chl was measured in THF (0.2 mM) at 100 K under illumination through the cavity window. The microwave power was 0.2 mW and the modulation amplitude was 16 G.

Light illumination was performed with continuous light from a 600-W tungsten lamp through a cold filter (Nihon Shinku Kogaku type-B) which passes the light of wavelengths shorter than 700 nm. The light intensity at the sample position was about 500 mW/cm^2.

RESULTS

FT-IR Difference Spectrum of $^3P_{680}/P_{680}$ in PS II RC. Figure 1A shows the FT-IR difference spectrum of PS II RC (D1–D2–cyt b–559 complex) between the before and under continuous-light illumination spectra at 80 K. As the D1–D2–cyt b–559 complex totally lacks the quinone acceptors, the charge-separated state ($P_{680}^+Pheo^-$) produced from the excited singlet state of P_{680} ($^1P_{680}^*$) recombines in about 50 ns and subsequently forms $^3P_{680}$ with a quantum yield of 0.6 (at 50 K) (Takahashi et al., 1987). This $^3P_{680}$ has a lifetime of 0.9 ms at 5–120 K (Takahashi et al., 1987). Although the triplet state of carotenoid is also formed with a low quantum yield (0.03), its formation is coupled with neither the charge recombination nor the $^3P_{680}$ relaxation; its rise time is about 12 ns and the decay time is 5–9 μs (Takahashi et al., 1987). From the quantum yields and the lifetimes of these transient species ($^1P_{680}^*$, $P_{680}^+Pheo^-$, $^3P_{680}$, and triplet carotenoid), we may reasonably consider that $^3P_{680}$ is the intermediate predominantly accumulated under continuous-light illumination. Thus, the spectrum in Figure 1A should exhibit the spectral change due to the formation of $^3P_{680}$ from ground-state P_{680}.

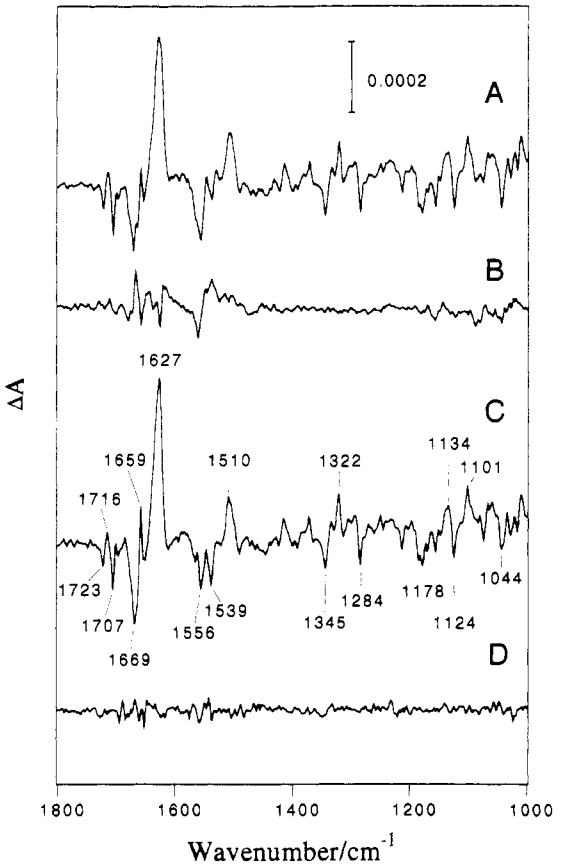

FIGURE 1: Light-induced FT-IR difference spectra of PS II RC (D1–D2–cyt *b*–559 complex) measured at 80 K. (A) FT-IR difference spectrum between before and under illumination. (B) FT-IR difference spectrum between before and after illumination. (C) FT-IR difference spectrum between P_{680} and $^3P_{680}$, which was obtained by subtraction of B from A (i.e., identical to the difference spectrum of under-minus-after illumination). (D) FT-IR difference spectrum of the denatured RC complex, which was obtained by the same procedures as C. Illumination was performed by continuous white light (<700 nm) with an intensity of about 500 mW/cm^{-2} at the sample point. Spectral resolution was 4 cm^{-1}.

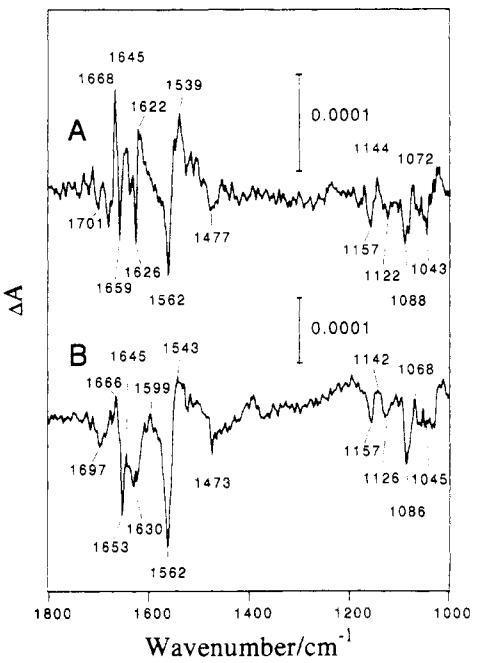

FIGURE 2: (A) FT-IR difference spectrum of RC between before and after illumination measured at 80 K. The spectrum is the same as that in Figure 1B except for the expanded absorbance scale. (B) FT-IR difference spectrum of RC obtained by increasing the sample temperature. The difference spectrum was measured while the temperature was increased from 80 to 81 K in a cryostat with a temperature controller.

If the RC sample contains neither exogenous reductants nor oxidants, any long-lived radical species would not remain stabilized after illumination. As a matter of fact, however, several bands were observed in the difference spectrum taken after illumination (Figure 1B). The spectral intensities of these bands increased as the illumination time increased, implying that some changes other than $^3P_{680}$ formation occurred and accumulated in the sample to remain after illumination. The possibility of photodegradation, however, was ruled out by the observation that these bands completely relaxed in several minutes after illumination ceased.

The cause for the presence of remainder bands in the after illumination spectrum is given in Figure 2, where the spectrum of after-minus-before illumination (Figure 2A) (expanded spectrum of Figure 1B) is compared with the difference spectrum obtained by slightly increasing the temperature (Figure 2B). Figure 2B expresses so-called thermal bands which appear due to an increased population of higher vibrational levels upon raising the sample temperature. The bands in the 1500–1700 cm^{-1} region of Figure 2B are derived from the amide I (1600–1700 cm^{-1}) and amide II (~1550 cm^{-1}) bands of proteins, and the bands in 1000-1200 cm^{-1} are from the buffer (phosphate) and detergent (dodecyl maltoside) molecules. The similarity in whole spectral features between the two spectra (Figure 2A,B) indicates that the bands remaining after illumination are attributed to the temperature increase due to light absorption by pigments and subsequent nonradiative relaxation to diffuse the thermal energy to proteins and buffer media. The small inconsistency of the band features in 1500–1700 cm^{-1} may be due to the difference in local temperature of the proteins between after internal heating as a result of illumination (Figure 2A) and after external heating (Figure 2B).

On the basis of the above consideration, the true difference spectrum between P_{680} and $^3P_{680}$ ($^3P_{680}/P_{680}$) free from contamination of thermal bands can be obtained by subtracting Figure 1B (after-minus-before illumination) from Figure 1A (under-minus-before illumination). In Figure 1C is shown that $^3P_{680}/P_{680}$ spectrum thus obtained. The negative peaks mean the bleaching of ground-state P_{680}, whereas the positive peaks mean the formation of $^3P_{680}$. The features of this spectrum are characterized by three negative peaks at 1723, 1707, and 1669 cm^{-1} and three positive peaks at 1716, 1659, and 1627 cm^{-1} in the region above 1600 cm^{-1}, two negative peaks at 1556 and 1539 cm^{-1} with one positive peak at 1510 cm^{-1} in the 1500–1600 cm^{-1} region, and many peaks with medium and low intensities in the region below 1400 cm^{-1}.

FT-IR Difference Spectra of T_1/S_0 in Purified Chl. In order to analyze the $^3P_{680}/P_{680}$ difference spectrum, FT-IR difference spectra between the S_0 and T_1 states (T_1/S_0) of purified Chl in organic solvents were investigated. Figure 3A shows a T_1/S_0 difference spectrum of Chl in THF (10^{-2} M) measured under the same illumination and temperature conditions as those employed for measuring the $^3P_{680}/P_{680}$ spectrum. Thermal bands of the solvent were canceled by subtracting the after illumination spectrum. The formation of T_1 was confirmed by ESR measurements under the conditions close to those of the FT-IR measurements: 2×10^{-4} M Chl in THF, under white light (<700 nm) illumination with an intensity of ca. 500 mW/cm^2 at 100 K. The resultant ESR spectrum exhibited a typical band pattern of T_1 Chl in organic solvents with the zero-field splitting parameters $|D|$ =

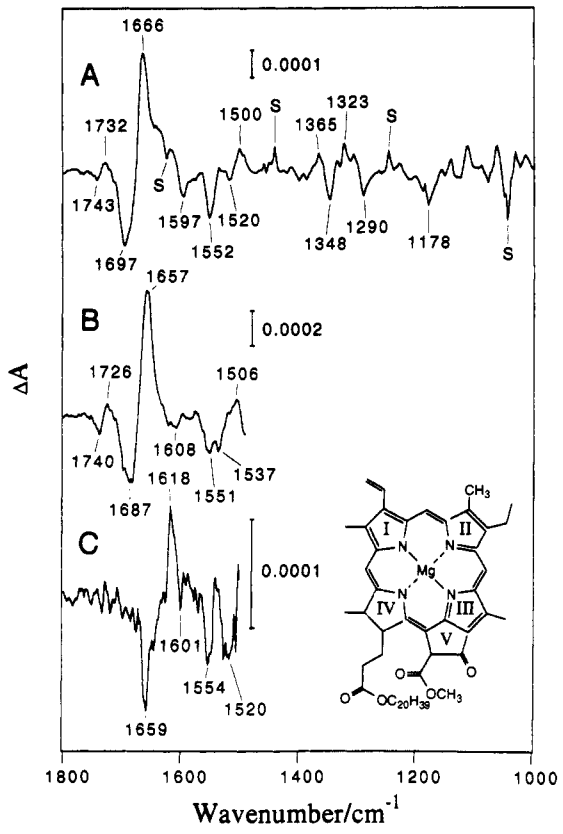

FIGURE 3: Light-induced FT-IR difference spectra between the S_0 and T_1 states of purified chlorophyll *a* (10^{-2} M) in tetrahydrofuran (A), triethylamine (B), and ethanol (C) measured at 80 K. Difference spectra between before and under illumination and spectra between before and after illumination were measured, and the latter were subtracted from the former so as to cancel the solvent thermal bands. Illumination conditions were the same as those in Figure 1. "S" indicates solvent peaks left to be subtracted. In B and C, the lower frequency region was not observable because of saturated solvent absorption. The inset shows the structure of chlorophyll *a*.

286×10^{-4} cm^{-1} and $|E| = 39 \times 10^{-4}$ cm^{-1} (spectrum not shown), which are in good agreement with those in the literature [summarized in Angerhofer (1991)].

The negative bands in Figure 3A, which reflect the IR bands of S_0 Chl, can be assigned with the aid of the literature [reviewed in Katz et al. (1966), Lutz (1984), Tasumi and Fujiwara (1987), Tasumi (1989), and Lutz and Mäntele (1991)]. The strongest band at 1697 cm^{-1} is unambiguously attributed to the C=O stretching mode of the keto C=O in ring V (see the Chl structure in the inset of Figure 3). The 1743 cm^{-1} band is assigned to either the ester C=O in ring V (carbomethoxy C=O) or that in ring IV (propionic acid C=O). In the T_1/S_0 difference spectrum, only the vibrational modes which change upon T_1 formation should appear. Hence, the carbomethoxy C=O located closer to the conjugated macrocycle, although not directly involved in conjugation, is more likely to be responsible for the 1743 cm^{-1} band. In fact, this assignment is consistent with the observation that, upon the formation of Chl cation (Chl^+), only the frequency of carbomethoxy C=O was affected while the propionic acid C=O was little affected (Nabedryk et al., 1990b). The bands at 1597, 1552, and 1520 cm^{-1} are assigned to the macrocycle C=C stretching modes, and the bands appearing in the region below 1400 cm^{-1} come from the mixed modes of macrocycle, stretches and deformations and C—H deformations. It is worth noting that the characteristics of these negative S_0 bands in the T_1/S_0 spectrum in THF are in good agreement with those in the Chl^+/Chl spectrum in the same solvent (Nabedryk et al., 1990b).

The IR spectra of T_1 Chl were obtained for the first time in this study. Although resonance Raman spectra of T_1 (B)-Chl have been previously obtained (Nishizawa et al., 1989; Kanzaki et al., 1990; Nishizawa & Koyama, 1990, 1991), C=O stretching modes have not been detected in these spectra. Further, in general resonance Raman-active modes of the macrocycle are rather different from the IR-active modes (Lutz & Mäntele, 1991). Thus, the present FT-IR spectra of T_1 Chl have provided the first observation of the C=O stretches and the IR-active macrocycle modes.

The most pronounced spectral changes associated with T_1 formation are the downshift of keto C=O from 1697 to 1666 cm^{-1}, the downshift of carbomethoxy C=O from 1743 to 1732 cm^{-1}, and the appearance of a band at 1500 cm^{-1} in the C=C stretching region (Figure 3A). The features of similar tendency were also observed in the T_1/S_0 difference spectra in TEA (Figure 3B) and EtOH solutions (Figure 3C). In these solvents, the spectra were observable only in the wavenumber region higher than 1490 (Figure 3B) and 1500 cm^{-1} (Figure 3C) because of the saturation of solvent bands in the lower wavenumber region. Spectral intensity was much lower in EtOH than in THF and TEA, probaby due to the shorter relaxation time of T_1 in EtOH. The downshift of the keto C=O band was observed as from 1687 to 1657 cm^{-1} in TEA and from 1659 to 1618 cm^{-1} in EtOH. Also, the downshift of the carbomethoxy C=O band was observed from 1740 to 1726 cm^{-1} in TEA, although in EtOH no corresponding bands could be detected due to low S/N. In the C=C stretching region, the features of spectral changes are more or less the same. In TEA, negative bands appeared at 1608, 1551, and 1537 cm^{-1} with a single positive band at 1506 cm^{-1}. Similarly, in EtOH three negative bands were observed at 1601, 1554, and 1520 cm^{-1}, although the positive band around 1500 cm^{-1} was not clearly resolved due to limitation in the detectable spectral region. The observation that only a single T_1 band appears instead of three S_0 bands in the C=C stretching region implies that the vibrational modes of macrocycle C=C stretches are significantly altered upon S_0-to-T_1 conversion.

Assignments of the Bands in the $^3P_{680}/P_{680}$ Difference Spectrum. When we compare the spectrum in Figure 1C with the spectra in Figure 3, it is clearly illustrated that the $^3P_{680}/P_{680}$ spectrum has most of the same features as the T_1/S_0 spectra of *in vitro* Chl. The 1669 cm^{-1} band that is assigned to the keto C=O stretching mode is downshifted to 1627 cm^{-1}, and the 1723 cm^{-1} band that is assignable to carbomethoxy C=O is downshifted to 1716 cm^{-1}. In the C=C stretching region, two bands at 1556 and 1539 cm^{-1} decrease and a new band appears at 1510 cm^{-1}. Also, in the lower frequency region, the positions of some of the bands are identical or similar to those in the T_1/S_0 spectrum of Chl; the negative bands at 1345, 1284, and 1178 cm^{-1} and the positive band at 1322 cm^{-1} in the $^3P_{680}/P_{680}$ spectrum (Figure 1C) correspond to the negative bands at 1348, 1290, and 1178 cm^{-1} and the positive band at 1323 cm^{-1} in the T_1/S_0 spectrum in THF (Figure 3A), respectively.

The pronounced differences in the features between the $^3P_{680}/P_{680}$ and T_1/S_0 spectra are the negative band at 1707 cm^{-1} and the positive band at 1659 cm^{-1}, both appearing in the C=O stretching region. At a glance, these bands would be ascribed to structural changes of apoproteins, e.g., by assigning the 1707 cm^{-1} band to the C=O stretch of a carboxylic acid group in Glu or Asp and the 1659 cm^{-1} band

to the C=O stretch of a backbone amide. It is generally expected, however, that the small perturbation in the protein structure upon $^3P_{680}$ formation will result in spectral bands of differential form. As opposed to this expectation, the two bands at 1707 and 1659 cm^{-1} have no corresponding partners, implying that these two bands do not originate from the structural perturbation of proteins. There is more evidence against the assignment of the 1707 cm^{-1} band to proteins: It has been shown that the C=O stretching frequency of a carboxylic acid group downshifts by about 10 cm^{-1} upon H–D exchange (Siebert et al., 1982). However, our FT-IR difference spectrum of RC in D_2O buffer exhibited no such shift; the position and the intensity of the 1707 cm^{-1} band were exactly the same as those in H_2O buffer (data not shown). It is thus inferred that the 1707 cm^{-1} band is not derived from a carboxylic acid group in the protein, although the possibility might remain that H–D exchange was insufficient due to the hydrophobicity of the proteins and/or the low temperature of incubation (4 °C). On the basis of these considerations, we conclude that the assignments of these two bands to structural changes of apoproteins are unlikely.

A straightforward interpretation of the two bands would be T_1 formation on another Chl molecule that is simultaneously involved in the $^3P_{680}$ formation. The 1707 and 1659 cm^{-1} bands can be assigned to the keto C=O stretches of the S_0 and T_1 states, respectively, and this downshift by 48 cm^{-1} is comparable to the downshift by 42 cm^{-1} (from 1669 to 1627 cm^{-1}) of the major keto C=O band. Also, the ratio of area intensities for these two pairs of bands exhibits similar values of 6.5 and 5.8 for ground-state bleaching (I_{1669}/I_{1707}) and triplet formation (I_{1627}/I_{1659}), respectively.

If the above interpretation is correct, which Chl (or Pheo) molecule is responsible for the minor C=O bands? Participation of Chl in denatured RC that might contaminate our RC sample was proved to be unlikely by the experiment using a totally denatured RC sample. As shown in Figure 1D, the FT-IR difference spectrum of the denatured sample measured with the same procedures as those used for the $^3P_{680}/P_{680}$ spectrum (Figure 1C) did not show any bands over the whole region. This is probably because in denatured RC the T_1 state of Chl is formed by direct intersystem crossing, so that the triplet yield is much lower than that of $^3P_{680}$ formation by the charge recombination mechanism. This suggests in turn that triplet formation by direct intersystem crossing in active RC will be negligibly small. In fact, this type of triplet formation by intersystem crossing, which would result in a spin-polarization pattern different from $^3P_{680}$, has not been reported in any of the ESR studies of $^3P_{680}$ (Rutherford et al., 1981; Rutherford, 1985; Ghanotakis et al., 1989; Van Mieghem et al., 1991).

Thus, the T_1 formation responsible for the minor 1707 and 1659 cm^{-1} bands must be directly coupled to $^3P_{680}$ formation. The simplest explanation is the contribution by another Chl in P_{680}; in other words, P_{680} is a Chl dimer in which the T_1 state, when formed, is mostly localized on one Chl molecule to exhibit the major 1669 and 1627 cm^{-1} bands, whereas the small portion of T_1 distributes on the other Chl molecule to exhibit the minor 1707 and 1659 cm^{-1} bands.

Another possibility, that the T_1 state on P_{680} migrates to accessory Chl or Pheo, can be examined by comparing the ground-state keto C=O frequencies. According to the FT-IR difference spectrum between Pheo and $Pheo^-$ (Nabedryk et al., 1990a) and the resonance Raman spectra excited with 406- and 413-nm laser lines (Moënne-Loccoz et al., 1989), Pheo as a primary acceptor shows a keto C=O band at 1677 (by FT-IR) or 1680 cm^{-1} (by Raman) and the other redox-inactive Pheo shows a band at 1701 cm^{-1} (by Raman). These frequencies do not agree with 1707 and 1669 cm^{-1} observed in the present $^3P_{680}/P_{680}$ spectrum, suggesting that Pheo is not related to these bands. This interpretation in turn implies that T_1 Pheo is not detected in the FT-IR difference spectrum at 80 K. Recently, Van der Vos et al. (1992) observed T_1 Pheo as a minor component (5–10% of $^3P_{680}$) at 1.2 K by ADMR spectroscopy. However, our temperature dependence experiment and calculations using its results suggest that the chemical species responsible for the minor 1707 and 1659 cm^{-1} bands should have almost no population at 1.2 K (less than 0.1% of the chemical species for the major 1669 and 1627 cm^{-1} bands) (see below). Van der Vos et al. (1992) also concluded that T_1 Pheo observed at 1.2 K is not likely to be formed by triplet energy transfer from $^3P_{680}$, but by singlet excitation trapping in Pheo when P_{680} is in the T_1 state. This mechanism of T_1 formation is clearly different from the case of the minor species in this study, which is in triplets energy transfer equilibrium with the major T_1 species (see below). Thus, the minor 1659/1707 cm^{-1} component does not appear identical to T_1 Pheo observed at 1.2 K. Probably, T_1 Pheo does not form at 80 K, at which temperature the yield of $^3P_{680}$ formation is lower and the decay time constant of T_1 Pheo is faster than these values at 1.2 K, or T_1 Pheo is created only in certain conditions of sample and illumination.

The frequency of the keto C=O band of accessory Chl was examined by utilizing the photooxidation of Chl by P_{680}, which occurs when cyt *b*–559 is already oxidized (Visser & Rijgersberg, 1974). The Chl^+/Chl difference FT-IR spectra were measured between before and after illumination at 210 K with Mn-depleted (by NH_2OH treatment followed by several washes) PS II membranes and also at 250 K with the D1–D2–cyt *b*–559 complex, in the presence of potassium ferricyanide (T. Noguchi, unpublished results). In both cases, the spectra exhibited negative bands at around 1680 and 1658 cm^{-1}, which are possible candidates for the keto C=O frequency of accessory Chl, but no bands at 1707 and 1669 cm^{-1}. This indicates that $^3P_{680}$ formation does not involve any T_1 state arising from redox-active accessory Chl. The possibility of migration of the triplet state to redox-inactive accessory Chl molecules is also unlikely because the coupling between these Chl molecules and P_{680} may be very weak.

In conclusion, the most probable interpretation is that P_{680} has a dimeric structure and $^3P_{680}$ is a T_1 state equilibrated between these two Chl molecules. At 80 K the T_1 state is mostly localized on one Chl; by comparing the area intensities between the major and minor keto C=O bands, the population ratio of the equilibrated triplet was calculated to be 0.86:0.14 (the average of 0.87:0.13 and 0.85:0.15 obtained for P_{680} bleaching and $^3P_{680}$ formation, respectively). The above view is further supported by examining the temperature dependence of the intensity ratios of the four keto C=O bands (see below).

Interactions of P_{680} and in Vitro Chl with Surrounding Molecules. Table I summarizes the band positions in the C=O and C=C stretching regions observed in the $^3P_{680}/P_{680}$ spectrum of RC and the T_1/S_0 spectra of *in vitro* Chl. In the carbomethoxy C=O region, S_0 Chl shows bands at 1743 and 1740 cm^{-1} in THF and TEA, respectively, and P_{680} shows a band at 1723 cm^{-1} (Table I). In general, the carbomethoxy C=O mode has a band in 1710–1750 cm^{-1} (Katz et al., 1966; Bekarek et al., 1979), and when it forms a hydrogen bond, the band appears at a lower frequency, e.g., at 1715 cm^{-1} in EtOH (Katz et al., 1966). The band positions at relatively higher frequencies in THF and TEA solutions (~1740 cm^{-1}) seen

Table I: Peak Positions (cm^{-1}) and Assignments of FT-IR Bands in the C=O and C=C Stretching Regions in the Triplet-Minus-Singlet Difference Spectra of Chlorophyll *a* in P_{680} and *in Vitro* Measured at 80 K

PC II RC		tetrahydrofuran		triethylamine		ethanol		
P_{680}	$^3P_{680}$	S_0	T_1	S_0	T_1	S_0	T_1	assignments
1723	1716(−7)[a]	1743	1732(−11)	1740	1726(−14)			carbomethoxy C=O stretch
1707 1669	1659(−48) 1627(−42)	1697	1666(−31)	1687	1657(−30)	1659	1618(−41)	keto C=O stretch
1612? 1556 1539[5][b]		1597[6] 1552 1520[6]		1608[5] 1551 1537[5]		1601[6] 1554 1520[6]		macrocycle C=C stretch
	1510[5]		1500[6]		1506[5]			

[a] Figures in parentheses indicate the band shift from the ground state to the triplet state. [b] Figures in square brackets indicate the coordination number obtained from the marker bands.

in the present study are consistent with the fact that these two solvents do not form hydrogen bonds. In contrast, the band position of P_{680} at 1723 cm^{-1} is low enough to consider the carbomethoxy C=O in P_{680} to be hydrogen-bonded. When we compare the intensity of this carbomethoxy C=O band relative to the keto C=O band between the $^3P_{680}/P_{680}$ spectrum (Figure 1C) and the T_1/S_0 spectra of *in vitro* Chl (Figure 3), the 1723 cm^{-1} band is clearly assigned to originate from the Chl molecule that is responsible for the major keto C=O band at 1669 cm^{-1}. In view of the dimeric structure of P_{680}, another carbomethoxy C=O band is expected to appear, but no such band could be found in the $^3P_{680}/P_{680}$ spectrum (Figure 1C). Judging from the intensity of the minor keto C=O band at 1707 cm^{-1}, the intensity of this carbomethoxy band should be higher than the noise level seen in 1730-1800 cm^{-1}. Accordingly, the reasonable interpretation is that the carbomethoxy C=O band associated with the minor keto C=O band at 1707 cm^{-1} is superimposed on the 1723 cm^{-1} band. On the basis of these considerations, we adopt the view that both carbomethoxy groups of the Chl molecules in P_{680} are hydrogen-bonded.

Solvent effects on the keto C=O frequency have been studied in detail by both IR and resonance Raman spectroscopies (Katz et al., 1966; Bekarek et al., 1979; Koyama et al., 1986; Krawczk, 1989). Chl in protic solvents exhibits a keto C=O band at 1660-1680 cm^{-1} and at 1680-1710 cm^{-1} in nonprotic solvents (Koyama et al., 1986; Krawczk, 1989). In fact, the keto C=O band of Chl in THF and TEA, nonprotic solvents, was found at 1697 and 1687 cm^{-1}, respectively, and that in EtOH, a protic solvent, was found at 1659 cm^{-1} (Table I). Employing the above criteria, we conclude that the keto C=O in P_{680} exhibiting the major band at 1669 cm^{-1} is hydrogen-bonded. It has also been shown that the keto C=O frequency linearly downshifts among nonprotic solvents with the parameter $(\epsilon - 1)(\nu^2 - 1)/(2\epsilon + 1)(2\nu^2 + 1)$, in which ϵ and ν stand for the relative dielectric constant and refractive index of a solvent, respectively (Bekarek et al., 1979; Krawczyk, 1989). A value of 1711 cm^{-1} has been obtained by an interpolation assuming no interactions with surroundings, i.e., in the ideal gas state (Bekarek et al., 1979; Krawczyk, 1989). Notably, the frequency of 1707 cm^{-1} observed in our $^3P_{680}/P_{680}$ spectrum (Table I) is close to this value, indicating that the keto C=O of one of the two Chl molecules is located in a highly nonpolar environment with almost no interaction with amino acid residues.

Some of the macrocycle C=C stretching bands appearing between 1500 and 1610 cm^{-1} can be used as markers for determining the coordination state of central Mg. It has been shown that the IR bands at ~1610 and ~1535 cm^{-1} in 5-coordinated Chl are downshifted to ~1600 and ~1515 cm^{-1}, respectively, in 6-coordinated Chl (Fujiwara & Tasumi, 1986; Tasumi & Fujiwara, 1987; Tasumi, 1989). In the present experiments, *in vitro* Chl in the S_0 state showed 6-coordinate characteristics in THF and EtOH, but 5-coordinate characteristics in TEA (Table I). This result partly contradicts a previous report that Chl is 5-coordinate in EtOH at room temperature (Fujiwara & Tasumi, 1986). The discrepancy probably comes from the coordination number change depending on the temperature (note that our measurements were done at 80 K). The phenomenon of coordination change from 5 to 6 at low temperatures has already been observed in diethyl ether solution (Krawczyk, 1989).

The band of T_1 Chl appears at 1500 cm^{-1} in THF and at 1506 cm^{-1} in TEA (Table I). Since Chl in the S_0 state takes the 6- and 5-coordinate states in the former and latter solvents, respectively, this frequency difference may be ascribed to the difference in coordination states of T_1 Chl. Thus, this IR-active mode will be a new marker band to discriminate the coordination number of T_1 Chl. In the $^3P_{680}/P_{680}$ spectrum, a negative band at 1539 cm^{-1} and a positive band at 1510 cm^{-1} were observed, indicating that the Chl molecules in P_{680} are 5-coordinate in both the S_0 and T_1 states (Table I). Although another marker band of coordination in the 1600–1610 cm^{-1} region was not clear in the $^3P_{680}/P_{680}$ spectrum, a dip at 1612 cm^{-1} underlying the foot of the large 1627 cm^{-1} band might be the concerned band (Figure 1C).

Temperature Dependence of the $^3P_{680}/P_{680}$ Spectrum. If the triplet state is equilibrated between the two Chl molecules in P_{680} as proposed above, the population ratio of the triplet between the two should be affected by the temperature change. Figure 4 shows the temperature dependence of the $^3P_{680}/P_{680}$ difference spectra in the C=O stretching region. The overall band intensity decreased as the temperature increased (Figure 4), in agreement with the decrease in the quantum yield of $^3P_{680}$ formation and in its lifetime with the temperature increase (Takahashi et al., 1987). In Figure 5, the area intensity ratio of the two negative bands of P_{680} at 1707 and 1669 cm^{-1} and the ratio of the two positive bands of $^3P_{680}$ at 1659 and 1627 cm^{-1} were calculated and expressed as an Arrhenius plot. In estimation of the area intensities, base lines expressed in Figure 4 were used, and the overlapping parts of the 1669 and 1659 cm^{-1} bands were taken into consideration. As seen in Figure 5, the ratio calculated for P_{680} bleaching is almost the same as that for $^3P_{680}$ formation, and all of the data points are well-fit to a linear regression line. From the slope of the line, the energy gap between the two Chl triplet states (ΔE) was calculated as $\Delta E = 8.4 \pm 0.7$ meV.

DISCUSSION

In spite of the similarities in amino acid sequences and photochemistry between PS II and bacterial RCs, the structure

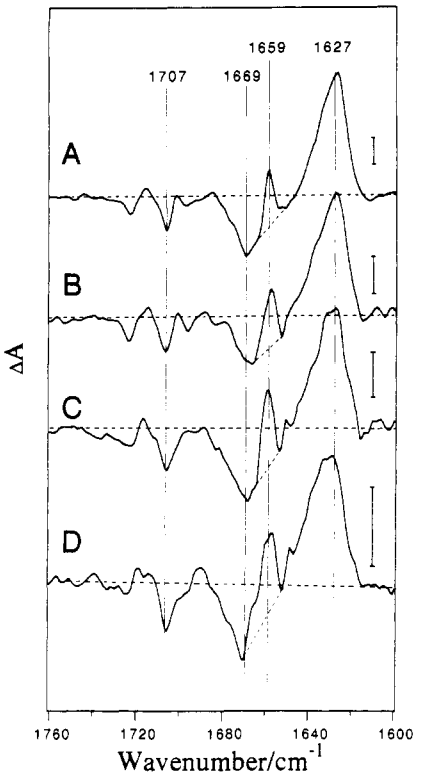

FIGURE 4: Temperature dependence of the $^3P_{680}/P_{680}$ difference spectra in the C=O stretching region: (A) 80, (B) 95, (C) 120, and (D) 160 K. The illumination conditions and the subtraction procedure were the same as those for obtaining the spectrum in Figure 1C. The scale bars indicate $\Delta A = 0.0001$. Base lines used for the calculation of area intensities of the four keto C=O bands marked (Figure 5) are expressed as broken lines.

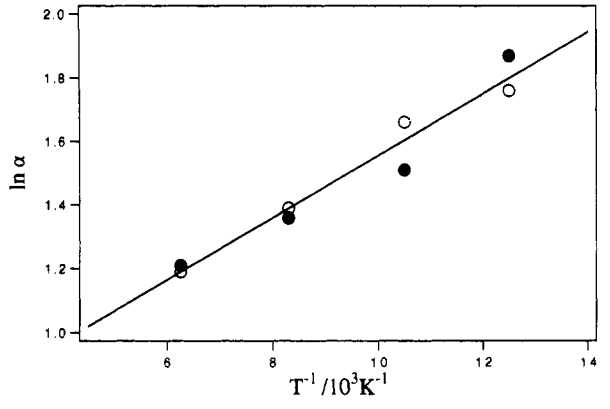

FIGURE 5: Relationship of the area intensity ratio (α) with the temperature: $\alpha = I_{1669}/I_{1707}$ for the negative P_{680} bands (●) and $\alpha = I_{1627}/I_{1659}$ for the positive $^3P_{680}$ bands (○). The line was obtained by a least-squares fitting.

of the PS II primary electron donor, P_{680}, has been under debate. Many investigators have argued dimeric and monomeric structures from their own standpoints (Van Gorkom et al., 1974; Davis et al., 1979; Den Blanken et al., 1983; Lösche et al., 1988; Ghanotakis et al., 1989; Tetenkin et al., 1989; Braun et al., 1990; Durrant et al., 1990; Moënne-Loccoz et al., 1990; Van Kan et al., 1990; Van Mieghem et al., 1991; Kwa et al., 1992; Otte et al., 1992; Van der Vos et al., 1992). However, since the red absorption bands of the chlorin compounds in RC, 6 Chl and 2 Pheo (Kobayashi et al., 1990), significantly overlap each other as they are more or less coupled, spectroscopic studies utilizing these electronic transitions, such as absorption difference, circular dichroism, fluorescence, and ADMR (Den Blanken et al., 1983; Tetenkin et al., 1989; Van Kan et al., 1990; Braun et al., 1990; Durrant et al., 1990; Kwa et al., 1992; Otte et al., 1992; Van der Vos et al., 1992), basically make it difficult to draw a clear conclusion. Also, in ESR spectroscopy, the bandwidth of P_{680}^+ (Van Gorkom et al., 1974) and the zero-field splitting parameters of $^3P_{680}$ (Rutherford et al., 1981; Ghanotakis et al., 1989) have been claimed to not decisively discriminate between dimeric and monomeric structures (Davis et al., 1979; Rutherford et al., 1981; Den Blanken et al., 1983). Furthermore, in most of the arguments, the definitions of monomer and dimer were rather ambiguous: Does a triplet localized on a single Chl molecule mean a monomer? What range of strength in the exciton coupling justifies a dimer? And so on. In these circumstances, the points to be questioned about P_{680} may be rearranged as follows: (1) Are there two Chl molecules corresponding to the bacterial special pair conserved in PS II RC? (2) Does P_{680} reside on such a pair of Chl or on another Chl? (3) Does the T_1 state stay on P_{680} or migrate to the other Chl? (4) If two Chl molecules are involved in P_{680}, how strongly are they coupled? (5) What is the cause for the high redox potential of P_{680}?

By employing FT-IR difference spectroscopy, some of these questions have been clearly answered. Our light-induced FT-IR difference spectrum of RC upon triplet formation exhibited two negative peaks at 1669 and 1707 cm^{-1}, both of which were assigned to the keto C=O stretches of the two Chl molecules (Figure 1C). Since these bands are not derived from the triplet formation by direct intersystem crossing, and since the band positions are obviously different from those of Pheo (Nabedryk et al., 1990a; Moënne-Loccoz et al., 1989) and accessory Chl coupled to P_{680} (T. Noguchi, unpublished data) in RC, neither Pheo nor Chl molecules other than P_{680} could be involved in triplet formation. In other words, the triplet state resides on P_{680} itself and does not migrate to any other places. This conclusion together with the obervation that two keto C=O bands appear upon triplet formation leads to a further conclusion that P_{680} consists of two Chl molecules; namely, a special pair-like structure is conserved in PS II RC, and P_{680} is located on this Chl dimer.

The keto C=O bands of the ground-state P_{680} at 1707 and 1669 cm^{-1} downshift to 1659 and 1627 cm^{-1}, respectively, upon conversion to $^3P_{680}$ (Table I). The values downshifted by 48 and 42 cm^{-1} are comparable with or larger than those found in the T_1/S_0 spectra of *in vitro* monomeric Chl: 31 cm^{-1} in THF, 30 cm^{-1} in TEA, and 41 cm^{-1} in EtOH (Table I). This result implies that the T_1 state in the P_{680} dimer is localized on either Chl molecule on a sub-picosecond time scale, the time resolution of IR spectroscopy, and is moving between the two Chl molecules on a larger time scale; if the T_1 state were originally delocalized within the dimer or were exchanging faster than sub-picoseconds, the band shift value would be much smaller than that in monomeric Chl. This idea is also supported by the unequivalent band intensities between the two Chl molecules (1669 and 1627 cm^{-1} pair vs 1707 and 1659 cm^{-1} pair, Figures 1C and 4): if the above assumption of original delocalization or faster triplet exchange were the case, the band intensities would be the same. From the intensity ratio of these keto C=O bands, distribution of the triplet population within the two Chl molecules in P_{680} was calculated to be 0.86:0.14 at 80 K (Figure 4). Also, from its temperature dependence, the energy gap between the two T_1 states localized on each of the Chl molecules is calculated to be 8.4 ± 0.7 meV (Figure 5). In conclusion, FT-IR spectroscopy has provided a view that P_{680} is a Chl dimer in which the T_1 state is equilibrated between the two Chl

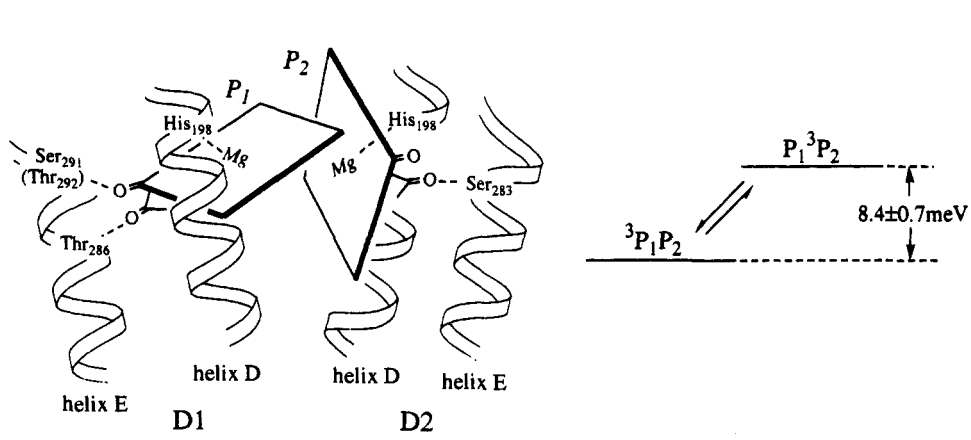

FIGURE 6: (Left) Structural model of P_{680} in PS II RC. The present FT-IR study has shown the dimeric structure, 5-coordination, and hydrogen-bonding properties of the keto and carbomethoxy C=O groups. Interactions of P_{680} with the specific amino acid residues in the D1 and D2 subunits were deduced from the sequence homology with the L and M subunits of *Rps. viridis* and *Rb. sphaeroides*. The triplet *z* axis tilted by 30° to the membrane plane that was claimed by Van Mieghem et al. (1991) was taken into consideration in the angle between the Chl attached to D1 (P_1) and the Chl attached to D2 (P_2) in this model. (Right) Relationship between the triplet state localized on P_1 and that on P_2. The two states are equilibrated with each other, and the energy gap was calculated to be 8.4 ± 0.7 meV.

molecules and its population is mostly distributed to one of them.

The result obtained in this study is consistent with the previous Raman data by Moënne-Loccoz et al. (1990), although the conclusion drawn is different. They measured resonance Raman spectra of PS II RC with high- and low-power excitation. By taking the difference between the two spectra, they observed P_{680} bleaching, which gave rise to only a single band at 1672 cm^{-1} assignable to keto C=O, and concluded that only one Chl is likely to be involved in the triplet formation (Moënne-Loccoz et al., 1990). The position of this band is virtually the same as that obtained in the present FT-IR study at 1669 cm^{-1} (spectral resolution is 4 cm^{-1}) as the major P_{680} bleaching band. Notably, their Raman spectra were measured at such a low temperature of 15 K that the population of the higher T_1 state calculated on the basis of the above-mentioned energy gap (8.4 ± 0.7 meV) is at most 0.1%, far lower than the discernible level. They probably observed only one of the two bands because of this extremely low temperature.

From the band positions of C=O and macrocycle C=C stretching modes, interactions of Chl with surrounding molecules can be examined. The C=C stretching bands of our spectrum indicated that the Chl molecules in P_{680} are 5-coordinate, in agreement with the conclusion derived from resonance Raman measurements by Moënne-Loccoz et al. (1990). This idea is reasonable in view of the fact that the two histidine residues coordinating to the special pair in bacterial RC are conserved in PS II (His D1–198 and His D2–198) (Trebst, 1986; Sayre et al., 1986; Michel & Deisenhofer, 1988).

In this study, the $^3P_{680}/P_{680}$ difference spectrum revealed that, among the two keto C=O groups in dimeric P_{680}, the one absorbing at 1669 cm^{-1} is hydrogen-bonded, while the other absorbing at 1707 cm^{-1} is free in a highly nonpolar environment. In *Rhodopseudomonas viridis*, the keto C=O of one of the special pair BChl, which is attached to the L subunit (P_L), forms a hydrogen bond with Thr L248, while the keto C=O of the other BChl attached to the M subunit (P_M) is free from a hydrogen bond (the adjacent residue is Ile M282) (Michel et al., 1986). In *Rhodobacter sphaeroides*, on the other hand, neither of the keto C=O groups are hydrogen-bonded (adjacent residues are Met L248 and Ile M284) (Yeates et al., 1988; El-Kabbani et al., 1991). Taking into account the advocated similarities in amino acid sequence and protein folding pattern between the D1 and D2 subunits in PS II and the L and M subunits in bacterial RC (Trebst, 1985; Sayre et al., 1986; Michel & Deisenhofer, 1988), we can assume the amino acid residues proximate to the keto C=O groups in P_{680} as follows: The residues in the D1 and D2 subunits corresponding to the bacterial residues adjacent to the keto C=O groups are Ile D1–290 and Val D2–287. Although both residues are not capable of hydrogen bonding, in D1 there are Ser D1–291 and Thr D1–292 next to Ile D1–290, while no hydrogen-bonding amino acids are found around Val D2–287 in D2. Thus, the most probable candidate for the amino acid residue that forms a hydrogen bond with one of the two keto C=O groups in P_{680} is Ser D1–291 or Thr D1–292. The fact that no hydrogen-bonding partner is found in D2 is in agreement with the FT-IR result that the keto C=O of the other Chl is located in a nonpolar environment.

In the carbomethoxy C=O region, only a single P_{680} band appeared at 1723 cm^{-1}, a frequency value which indicates hydrogen-bond formation (Figure 1C). On the basis of its intensity relative to the keto C=O bands, it is clear that the carbomethoxy C=O of the Chl molecule with hydrogen-bonded keto C=O is responsible for this band and forms a hydrogen bond. The carbomethoxy C=O band of the other Chl is supposed to be overlapping this 1723 cm^{-1} band, and hence this C=O may also be hydrogen-bonded. In *Rps. viridis*, Ser M203 in helix D forms a hydrogen bond with the carbomethoxy C=O of P_M BChl (Michel et al., 1986), while in *Rb. sphaeroides* Ser L244 in helix E hydrogen bonds to that of P_L (El-Kabbani et al., 1991). In PS II, Gly D1–201 and Gly D2–201 are the residues corresponding to Ser M203 of *Rps. viridis*, and Thr D1–286 and Ser D2–283 correspond with Ser L244 of *Rb. sphaeroides* (Trebst, 1985; Sayre et al., 1986; Michel & Deisenhofer, 1988). Since Gly cannot form a hydrogen bond, while Thr and Ser are capable of hydrogen bonding, it is readily supposed that Thr D1–286 and Ser D2–283 are the hydrogen-bonding partners of the two carbomethoxy C=O groups of P_{680}.

Figure 6 depicts a model of the P_{680} structure and its interactions with apoproteins that is obtained by summarizing the above discussion. P_{680} consists of a pair of Chl molecules; one Chl, attached to the D1 subunit (designated P_1), has a

keto C=O forming a hydrogen bond with Ser D1–291 or Thr D1–292 and a carbomethoxy C=O hydrogen-bonded with Thr D1–286. The other Chl, attached to the D2 subunit (designated P_2), has a keto C=O free from hydrogen bonding and a carbomethoxy C=C hydrogen-bonded with Ser D2–283. The T_1 state equilibrates between P_1 and P_2 with a population mostly distributed to P_1, which has a lower triplet energy level.

It has been proposed from ESR measurements that, in *Rps. viridis*, the T_1 state of the special pair is localized on P_L, while in *Rb. sphaeroides* it is equivalently distributed between both of the BChl molecules (Norris et al., 1989). El-Kabbani et al. (1991) have compared the hydrogen-bonding properties of the carbonyl groups of the BChl dimer between those in *Rps. viridis* and those in *Rb. sphaeroides* and have suggested that hydrogen bonding of keto C=O is important for the triplet localization: the keto C=O of P_L is hydrogen-bonded in *Rps. viridis*, while both of the keto C=O groups are free from a hydrogen bond in *Rb. sphaeroides*. This idea is in agreement with the triplet distribution and hydrogen-bonding pattern in PS II, which has been obtained by the present FT-IR study: P_1, in which the T_1 state is mostly distributed, has a hydrogen-bonded keto C=O, whereas P_2 has a free keto C=O.

Van Mieghem et al. (1991) showed by ESR measurements at 4.4 K using oriented PS II samples that the triplet *z* axis of $^3P_{680}$ is tilted by 30° to the membrane plane. On the basis of the prediction by our FT-IR measurements that the triplet state is almost completely localized only on P_1 at this extremely low temperature, it is deduced that the Chl molecule tilted by 30° to the membrane is P_1 itself. This P_1 arrangement significantly contrasts with the bacterial case, in which both of the BChl molecules in the special pair are arranged almost perpendicular to the membrane plane. This large arrangement change may be achieved by the rigid hydrogen-bond formation with surrounding proteins. Our FT-IR results indicated that both the keto and carbomethoxy C=O groups of P_1 form hydrogen bonds, whereas in *Rps. viridis* and *Rb. sphaeroides* the two C=O groups do not form hydrogen bonds at the same time (Michel et al., 1986; Yeates et al., 1988; El-Kabbani et al., 1991).

Furthermore, the amino acid residue supposed to form a hydrogen bond with the keto C=O of P_1 (Ser D1–291 or Thr D1–292) is shifted by one or two residues from Ile D1–290, corresponding to the residue adjacent to the keto C=O in bacteria. It is possible that this deviation causes the orientation change of P_1. Since in P_2 the keto C=O is not hydrogen-bonded and the carbomethoxy C=O probably forms a hydrogen bond with Ser D2-283, which exactly corresponds to the bacterial residue neighboring the carbomethoxy C=O, the P_2 arrangement may be conserved in PS II RC, i.e., P_2 is oriented perpendicular to the membrane plane. The possibility of this type of dimeric structure of P_{680}, in which one of the Chl molecules is oriented at 30° to the membrane plane, has been also pointed out by Van Mieghem et al. (1991) (although they favored another monomeric model). These P_1 and P_2 arrangements are also incorporated in the P_{680} model in Figure 6.

As a consequence of the arrangement of P_1 and P_2 discussed above, the dimeric structure of P_{680} appears considerably different from that of the bacterial primary donor. The Chl planes are no longer oriented parallel, and the angle between them is so large that the overlapping of the macrocycles will be much smaller. It is readily considered that this dimeric configuration causes a weaker exciton coupling, resulting in small band splitting in the red absorption spectrum. Also, it is likely that this asymmetric structure and the hydrogen-bonding characteristics of the Chl dimer are the reasons why P_{680} has a higher redox potential than other primary donors.

ACKNOWLEDGMENT

We thank Dr. T. Ono for valuable advice and helpful discussions.

REFERENCES

Allen, J. P., Feher, G., Yeates, T. O., Komiya, H., & Rees, D. C. (1987a) *Proc. Natl. Acad. Sci. U.S.A. 84*, 5730–5734.
Allen, J. P., Feher, G., Yeates, T. O., Komiya, H., & Rees, D. C. (1987b) *Proc. Natl. Acad. Sci. U.S.A. 84*, 6162–6166.
Angerhofer, A. (1991) in *Chlorophylls* (Scheer, H., Ed.) pp 945–991, CRC Press, Boca Raton, FL.
Barber, J., Chapman, D. J., & Telfer, A. (1987) *FEBS Lett. 220*, 67–73.
Bekarek, V., Kaplanova, M., & Socha, J. (1979) *Stud. Biophys. 77*, 21–24.
Braun, P., Greenberg, B. M., & Scherz, A. (1990) *Biochemistry 29*, 10376–10387.
Chang, C.-H., El-Kabbani, O., Tiede, D., Norris, J., & Schiffer, M. (1991) *Biochemistry 30*, 5352–5360.
Davis, M. S., Forman, A., & Fajer, J. (1979) *Proc. Natl. Acad. Sci. U.S.A. 76*, 4170–4174.
Deisenhofer, J., Epp, O., Miki, K., Huber, R., & Michel, H. (1984) *J. Mol. Biol. 180*, 385–398.
Deisenhofer, J., Epp, O., Miki, K., Huber, R., & Michel, H. (1985) *Nature 318*, 618–624.
Den Blanken, H. J., Hoff, A. J., Jongenelis, A. P. J. M., & Diner, B. A. (1983) *FEBS Lett. 157*, 21–27.
Durrant, J. R., Giorgi, L. B., Barber, J., Klug, D. R., & Porter, G. (1990) *Biochim. Biophys. Acta 1017*, 167–175.
El-Kabbani, O., Chang, C.-H., Tiede, D., Norris, J., & Schiffer, M. (1991) *Biochemistry 30*, 5361–5369.
Friesner, R. A., & Won, Y. (1989) *Biochim. Biophys. Acta 977*, 99–122.
Fujiwara, M., & Tasumi, M. (1986) *J. Phys. Chem. 90*, 250–255.
Ghanotakis, D. F., De Paula, J. C., Demetriou, D. M., Bowlby, N. R., Petersen, J., Babcock, G. T., & Yocum, C. F. (1989) *Biochim. Biophys. Acta 974*, 44–53.
Kanzaki, M., Yuzawa, T., Hiura, H., & Takahashi, H. (1990) *Chem. Phys. Lett. 169*, 85–88.
Katz, J. J., Dougherty, R. C., & Boucher, L. J. (1966) in *The Chlorophylls* (Vernon, L. P., & Seely, G. R., Eds.) pp 185–251, Academic Press, New York.
Kobayashi, M., Maeda, H., Watanabe, T., Nakane, H., & Satoh, K. (1990) *FEBS Lett. 260*, 138–140.
Koyama, Y., Umemoto, Y., & Akamatsu, A. (1986) *J. Mol. Struct. 146*, 273–287.
Krawczyk, S. (1989) *Biochim. Biophys. Acta 976*, 140–149.
Kwa, S. L. S., Newell, W. R., Van Grondelle, R., & Dekker, J. P. (1992) *Biochim. Biophys. Acta 1099*, 193–202.
Lösche, M., Satoh, K., Feher, G., & Okamura, M. Y. (1988) *Biophys. J. 53*, 270a.
Lutz, M. (1984) in *Advances in Infrared and Raman Spectroscopy* (Clark, R. J. H., & Hester, R. E., Eds.) Vol. 11 pp 211–300, Wiley, New York.
Lutz, M., & Mäntele, W. (1991) in *Chlorophylls* (Scheer, H., Ed.) pp 855–902, CRC Press, Boca Raton, FL.
Moënne-Loccoz, P., Robert, B., & Lutz, M. (1989) *Biochemistry 28*, 3641–3645.
Moënne-Loccoz, P., Robert, B., & Lutz, M. (1990) in *Current Research in Photosynthesis* (Baltscheffsky, M., Ed.) Vol. I, pp 423–426, Kluwer Academic Publishers, Dordrecht, The Netherlands.
Michel, H., & Deisenhofer, J. (1988) *Biochemistry 27*, 1–7.

Michel, H., Epp, O., & Deisenhofer, J. (1986) *EMBO J. 5*, 2445–2451.

Nabedryk, E., Andrianambinintsoa, S., Berger, G., Leonhard, M., Mäntele, W., & Breton, J. (1990a) *Biochim. Biophys. Acta 1016*, 49–54.

Nabedryk, E., Leonhard, M., Mäntele, W., & Breton, J. (1990b) *Biochemistry 29*, 3242–3247.

Nanba, O., & Satoh, K. (1987) *Proc. Natl. Acad. Sci. U.S.A. 84*, 109–112.

Nishizawa, E., & Koyama, Y. (1990) *Chem. Phys. Lett. 172*, 317–322.

Nishizawa, E., & Koyama, Y. (1991) *Chem. Phys. Lett. 176*, 390–394.

Nishizawa, E., Hashimoto, H., & Koyama, Y. (1989) *Chem. Phys. Lett. 164*, 155–160.

Norris, J. R., Budil, D. E., Gast, P., Chang, C.-H., El-Kabbani, O., & Schiffer, M. (1989) *Proc. Natl. Acad. Sci. U.S.A. 86*, 4335–4339.

Omata, T., & Murata, N. (1980) *Photochem. Photobiol. 31*, 183–185.

Otte, S. C. M., Van der Vos, R., & Van Gorkom, H. J. (1992) *J. Photochem. Photobiol. B15*, 5–14.

Rutherford, A. W. (1985) *Biochim. Biophys. Acta 807*, 189–201.

Rutherford, A. W., Paterson, D. R., & Mullet, J. E. (1981) *Biochim. Biophys. Acta 635*, 205–214.

Sayre, R. T., Andersson, B., & Bogorad, L. (1986) *Cell 47*, 601–608.

Siebert, F., Mäntele, W., & Kreutz, W. (1982) *FEBS Lett. 141*, 82–87.

Takahashi, Y., Hansson, Ö., Mathis, P., & Satoh, K. (1987) *Biochim. Biophys. Acta 893*, 49–59.

Tasumi, M. (1989) in *Spectroscopy of Inorganic Bioactivators. Theory and Applications—Chemistry, Physics, Biology, and Medicine* (Theophanides, T., Ed.) pp 439–454, Kluwer Academic Publishers, Dordrecht, The Netherlands.

Tasumi, M., & Fujiwara, M. (1987) in *Spectroscopy of Inorganic-based Materials* (Clark, R. J. H., & Hester, R. E., Eds.) pp 407–428, John Wiley & Sons, Chichester, UK.

Tetenkin, V. L., Gulyaev, B. A., Seibert, M., & Rubin, A. B. (1989) *FEBS Lett. 250*, 459–463.

Trebst, A. (1986) *Z. Naturforsch. 41c*, 240–245.

Van der Vos, R., Van Leeuwen, P. J., Braun, P., & Hoff, A. J. (1992) *Biochim. Biophys. Acta 1140*, 184–198.

Van Gorkom, H. J., Tamminga, J. J., & Haveman, J. (1974) *Biochim. Biophys. Acta 347*, 417–438.

Van Kan, P. J. M., Otte, S. C. M., Kleinherenbrink, F. A. M., Nieveen, M. C., Aartsma, T. J., & Van Gorkom, H. J. (1990) *Biochim. Biophys. Acta 1020*, 146–152.

Van Mieghem, F. J. E., Satoh, K., & Rutherford, A. W. (1991) *Biochim. Biophys. Acta 1058*, 379–385.

Visser, J. W. M., & Rijgersberg, C. P. (1974) in *Proceedings of the International Congress on Photosynthesis, 3rd* (Avion, M., Ed.) pp 323–334, Elsevier, Amsterdam.

Yeates, T. O., Komiya, H., Chirino, A., Rees, D. C., Allen, J. P., & Feher, G. (1988) *Proc. Natl. Acad. Sci. U.S.A. 85*, 7993–7997.